Journal of Power Sources 195 (2010) 5052–5056

Contents lists available at ScienceDirect

Journal of Power Sources

journal homepage: www.elsevier.com/locate/jpowsour

Short communication

A novel carbon–silicon composite nanofiber prepared via electrospinning as anode material for high energy-density lithium ion batteries

L. Wang[a], C.X. Ding[a], L.C. Zhang[a], H.W. Xu[a], D.W. Zhang[a], T. Cheng[b], C.H. Chen[a,*]

[a] CAS Key Laboratory of Materials for Energy Conversion, Department of Materials Science and Engineering, University of Science and Technology of China, Anhui, Hefei 230026, China
[b] Nanjing University of Science and Technology, Jiangsu, Nanjing 210094, China

ARTICLE INFO

Article history:
Received 29 July 2009
Received in revised form 23 October 2009
Accepted 16 January 2010
Available online 23 February 2010

Keywords:
Silicon
Composite
Nanofiber
Electrospinning
Lithium ion battery

ABSTRACT

Electrospun carbon–silicon composite nanofiber is employed as anode material for lithium ion batteries. The morphology of composite nanofiber is optimized on the C/Si ratio to make sure well distribution of silicon particles in carbon matrix. The C/Si (77/23, w/w) nanofiber exhibits large reversible capacity up to 1240 mAh g^{-1} and excellent capacity retention. Ex situ scanning electron microscopy is also conducted to study the morphology change during discharge/charge cycle, and the result reveals that fibrous morphology can effectively prevent the electrode from mechanical failure due to the large volume expansion during lithium insertion in silicon. AC impedance spectroscopy reveals the possible reason of unsatisfactory rate capability of the nanofiber. These results indicate that this novel C/Si composite nanofiber may has some limitations on high power lithium ion batteries, but it can be a very attractive potential anode material for high energy-density lithium-ion batteries.

1. Introduction

Thanks to their high energy density and long cycle life, lithium ion batteries are usually employed as the power sources for portable electronic devices, such as cell phone, camera, MP3. However, the state-of-the-art batteries with $LiCoO_2$ and carbonaceous materials as the positive and negative electrodes cannot satisfy the requirement to further enhance the portability, and it becomes increasingly important to develop new electrode materials with higher energy density. Recently, much attention is focused on searching for new anode materials to replace graphite, which has a theoretical capacity of 372 mAh g^{-1}. Among the candidates of new anode materials, silicon is rather attractive for its high gravimetric specific capacity (4200 mAh g^{-1}) to form Li–Si alloy [1,2]. Unfortunately, there is an approximately four times volume expansion when silicon is completely alloyed with lithium [2–4], resulting in a rapid capacity fade and short cycle life. Great efforts were made to improve the cycling performance of silicon in the last few years, and the preparation of silicon-based materials with a designed nanostructure and carbon–silicon composite seems to be a possible way to solve the problem because nanostructured materials have usually a large pore volume that allows the digestion of huge volume expansion without causing mechanical fracture or cracking.

Cui et al. found that silicon nanowires grown by vapor–liquid–solid method exhibit large reversible capacity up to 3100 mAh g^{-1} together with excellent capacity retention during the first 10 cycles [5]. Recently, they also reported CVD-grown silicon nanowires with crystalline-amorphous core-shell structure which exhibited stable cycling performance even in 100 cycles [6]. On the other hand, C/Si composite materials where carbon can buffer the volume expansion and enhance the electronic conductivity, seem to be much easier to be prepared than silicon nanowires [7–12]. Wolf et al. reported carbon–fiber–silicon-nanocomposites where silicon nanoparticles were deposited on the surface of carbon fibers by microwave plasma chemical vapor deposition, and the composite with 19 wt% silicon exhibited stable reversible capacity over 700 mAh g^{-1} [13]. Obviously, it is a practical way to combine 1D nanostructure and carbon composite to enhance the electrochemical performance of silicon. Last year, we reported an electrospun Fe_3O_4/C composite nanofiber which has remarkable advantages over bare Fe_3O_4/C nanoparticles [14]. The carbon matrix can effectively buffer the volume expansion of metal oxide during the lithium intercalation, preventing mechanical failure and resulting in improved cycle life. Therefore, here we present a novel electrospun C/Si composite nanofiber as an anode material for lithium batteries. The composite nanofiber exhibits good capacity retention and higher gravimetric specific capacity compared with other carbon/silicon composite with similar silicon ratio. The ex situ SEM investigation is also conducted to study the morphology change during the lithium intercalation.

* Corresponding author. Tel.: +86 551 3606971.
E-mail address: cchchen@ustc.edu.cn (C.H. Chen).

0378-7753/$ – see front matter © 2010 Elsevier B.V. All rights reserved.
doi:10.1016/j.jpowsour.2010.01.088

2. Experimental

About 0.75 g polyacrylonitrile (PAN) (M.W. 86,000) was dissolved in 10 mL N-N-dimethylformamide (DMF) to form a polymer precursor, then nano-sized silicon particles (~50 nm) were added into the polymer solution with different PAN/Si weight ratios of 6:1, 4:1, and 2:1. The suspensions were vigorously stirred for 1 h and then ultrasonically dispersed for 30 min to form homogenous brown suspensions. For a typical electrospinning process, a suspension was firstly transferred into a 1 mL syringe and supplied to a metal needle with a flow rate of 5 μL min^{-1} by a syringe pump. Thus, PAN/Si composite nanofiber was obtained by a typical electrospinning method as described in our early work [14,15]. The composite fiber was pre-oxidized at 240 °C in air for 6 h to protect the fibrous morphology during the subsequent carbonization. Then the pre-oxidized nanofiber was moved to a tube furnace and carbonated under Ar atmosphere at 600 °C for 8 h. The derived C/Si nanofiber was characterized by X-ray diffraction (Philips X'pert Pro Super, Cu Kα radiation). The morphology of this nanofiber was examined with a scanning electron microscope (SEM) (JEOL 6390-LA). The weight ratio of carbon and silicon was analyzed by X-ray energy dispersive spectra (EDX). The PAN/Si and derived C/Si composite nanofibers were characterized by Fourier transform infrared spectroscopy (Bruker EQUINOX55). The bare nano-sized silicon powder was also analyzed as a parallel sample for comparison.

The electrochemical properties of the C/Si composite nanofibers were characterized using 2032 coin cells with metallic lithium as the counter electrode. The C/Si composite nanofibers were adhered onto a copper foil with a PVDF binder to make working electrodes while the load density is about 1.3 mg cm^{-2}. The weight ratio of the active materials and the binder was controlled as 85:15. A mixture of acetylene black (AB) and nano-sized silicon with a weight ratio of 3:1 was used as the reference. The electrode of AB/Si mixture was prepared by blade-casting method and the thickness was controlled at about 50 μm. The electrolyte was 1 M $LiPF_6$ in ethylene carbonate/dimethyl carbonate (1:1, v/v). The cells were assembled in an argon-filled glove box (MBRAUN LABMASTER 130) with moisture and oxygen levels less than 1 ppm. They were cycled in the voltage range between 3.0 and 0 V on a multi-channel battery cycler (NEWWAEE BTS-610). The cyclic voltammogram and AC impedance spectra were measured with an electrochemical workstation (CHI 604b), and the frequency of AC impedance is from 0.01 to 10,000 Hz. Some of the cells were disassembled after electrochemical cycling and the nanofiber electrodes were washed by diethylene carbonate and N-methyl-pyrrolidone before they were observed by SEM.

3. Results and discussions

Fig. 1 shows the scanning electron microscope images of the C/Si composite fibers derived from polymer precursor with different PAN:Si mass ratios. When the silicon concentration is controlled at a relatively low level (PAN/Si = 6:1), most of the composite has a smooth fibrous morphology, except for a few large Si agglomerates dispersed in the carbon fiber matrix (Fig. 1a). The energy dispersive X-ray spectroscopy (EDX) results shows that the mass ratio of carbon and silicon is 77:23 (3.3:1), indicating an approximately 50% carbon yield of PAN. Due to the large volume shrinkage of PAN during thermal treatment, the nanofibers become a little curly, which has been also observed by Kim et al. in the case of pure carbon fiber [16]. It is also noticed that when the content of silicon increases, it becomes difficult to disperse the Si nanoparticles in the polymer solution, leading to lots of agglomerations in the final production (Fig. 1b and c). When PAN/Si = 2:1 (Fig. 1c), the products are full of agglomerates of several micrometers in size, and a very small fraction of carbon nanofibers. The situation becomes worse when the content of silicon is increased to PAN/Si = 2:1. Therefore, it is necessary to control the silicon content at a low level to obtain C/Si composites with homogeneous compositions, and all of the C/Si composite nanofiber referred below is derived from PAN/Si = 6:1, corresponding to weight ratio as C/Si = 3.3:1.

In order to obtain carbon nanofibers will have higher reversible capacity, the carbonization temperature is selected as 600 °C according to our early report [15]. Fig. 2 exhibits the FT-IR spectra of the composite nanofibers before and after the thermal treatment. The as-electrospun PAN/Si composite nanofiber (spectrum a) shows a spectrum that is composed of the typical absorption of PAN [17] and some small peaks near 1100 cm^{-1}, which can be assigned to the absorption of silicon nanoparticles (spectrum c). The three absorption peaks near 1150, 1620 and 3450 cm^{-1} are almost the same as those of a pure carbon nanofiber derived from PAN [14]. But the signals of silicon particles contained in the fiber cannot be distinguished because of the overlapping of the peaks. Hence it suggests that the PAN contained in the composite nanofiber is completely carbonized. Fig. 3 shows the XRD result of the composite nanofiber carbonized at 600 °C. The peaks at 28.4°, 47.3° and 56.2° correspond to the (1 1 1) (2 2 0) and (3 1 1) diffraction of silicon (JCPDS 772107). Therefore, the nano-sized silicon particles contained in the composite nanofiber should be crystalline. In addition to the diffraction of silicon, there are also two broad diffraction peaks near 24° and 55°, which should be related to the disordered carbon produced by the PAN carbonization [14].

Fig. 4 shows the cyclic voltammogram (CV) of C/Si nanofiber and AB/Si mixture (inset) during the first three charge–discharge cycles. The composite fiber exhibits different anodic and cathodic performance in the first cycle compared to the following cycles. A small anodic peak is measured near 1.3 V, and is from the lithium intercalation into disordered carbon that contained in the composite fiber. This process is reversible because a corresponding cathodic peak at 1.3 V is also observed. There is a primary anodic peak below 0.75 V during the 1st cycle, and it should be contributed together by the lithium intercalation into the carbon and silicon, and the formation of solid electrolyte interphase (SEI). Compared to the former peak, this peak has larger area, which means that most of the discharge capacity is delivered during this process. It is widely acknowledged that lithium can insert into silicon below 0.4 V [18] and can deliver a capacity of more than 2000 mAh g^{-1}, so this strong anodic peak is considered from the lithium intercalation to carbon fiber and alloying with silicon nanoparticles. Fig. 5 exhibits voltage profiles of C/Si fiber vs. Li and AB/Si vs. Li cells in the first two cycles. Similar to the CV results, there are several plateaus corresponding to different lithium insertion/extraction processes. Although the silicon content in the composite fiber is only 23 wt% according to the EDX analysis, the 1st cycle discharge capacity reaches 1710 mAh g^{-1}, which is much higher than that of the early reported CSi composite (weight ration of C/Si is 2:1) prepared by high energy mechanical milling [19]. The reversible capacity is 1240 mAh g^{-1}, indicating an initial columbic efficiency of 72.5%. The irreversible capacity loss in the 1st cycle can be ascribed to the presences of the SiO_2 layer on the surface of silicon nanoparticles [10] and the micropores on the surface of disordered carbon [20]. The voltage profiles of AB/Si mixture are also presented in Fig. 5. Basically, both of the C/Si nanofiber and AB/Si mixture exhibit similar voltage profiles in the first two cycles, but it seems that the carbon derived from PAN can accommodates more lithium compared with AB, because the plateau between 1 and 0.2 V of the composite nanofiber in the first cycle is substantially longer that of the mixture. Furthermore, the initial discharge/charge capacity of AB mixture is only 870 and 640 mAh g^{-1}, respectively, which is almost half of the C/Si nanofiber. Also, our early study showed that the capacity of pure PAN-derived nanofiber has a capacity of 800 mAh g^{-1}

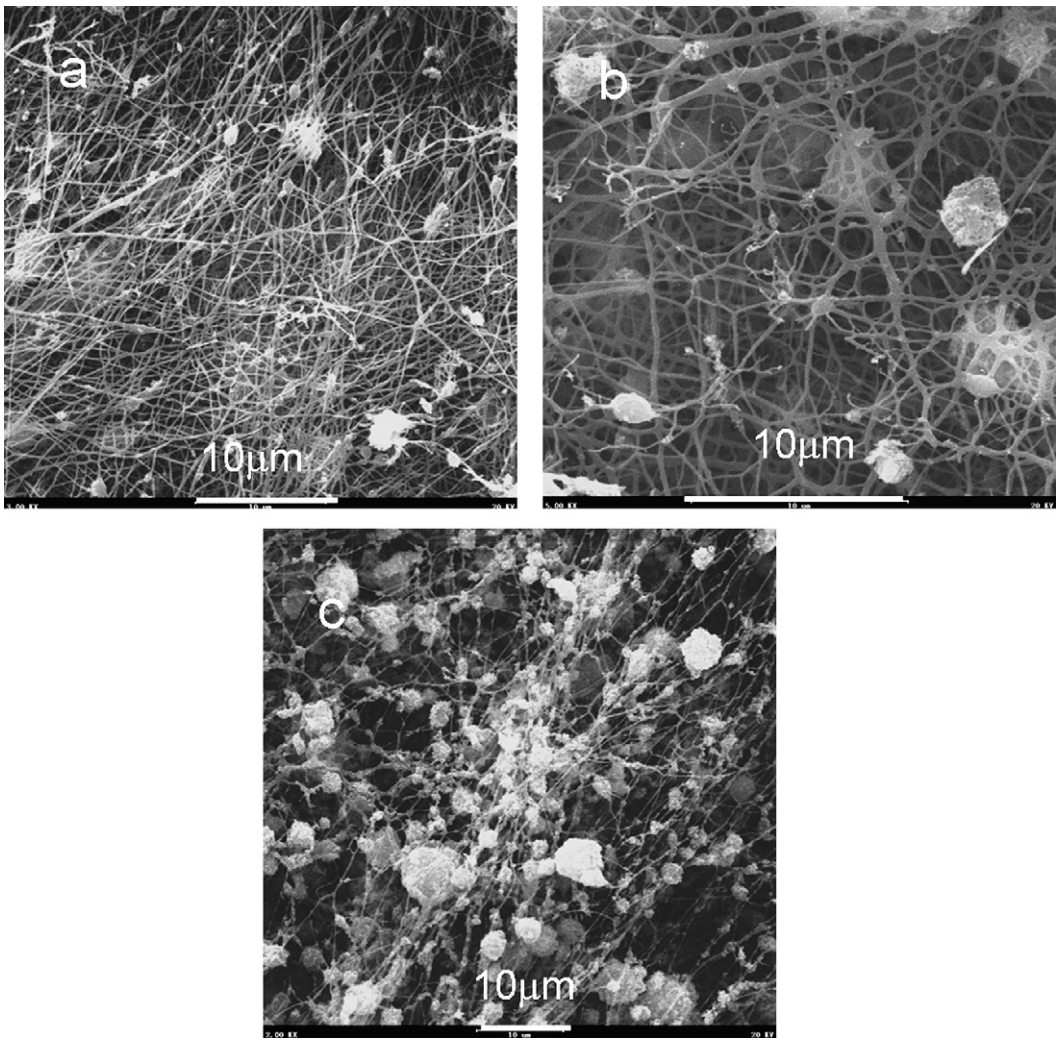

Fig. 1. SEM images of C/Si composite nanofibers derived from different PAN/Si ratios: (a) PAN/Si = 6:1; (b) PAN/Si = 4:1; (c) PAN/Si = 2:1.

at a similar current density [15], a rough estimation on the basis of 1240 mAh g^{-1} reversible capacity of the C/Si composite can be made here to reveal that 1 mole of silicon contained in the C/Si nanofiber can accommodate 3.2 mole of lithium on average.

The discharge capacity and columbic efficiency vs. cycle number are shown in Fig. 6. Compared with traditional silicon-based anode materials, which always have problem with long cycling, the C/Si composite fiber exhibits satisfactorily stable cycling performance. During the cycles at 0.1 C (1 C = 1500 mA g^{-1}), a slight

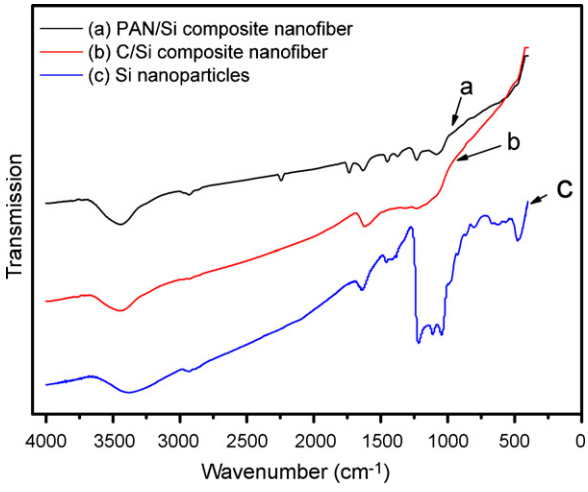

Fig. 2. Fourier transform infrared spectroscopy of pristine Si powder, electrospun PAN/Si = 6:1 nanofiber and derived C/Si = 3.3:1 nanofiber.

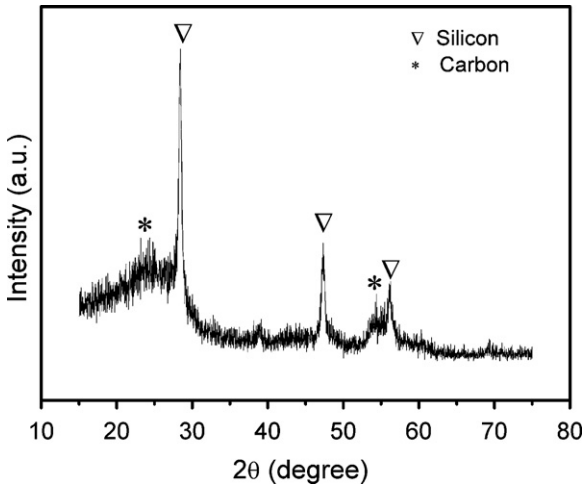

Fig. 3. XRD pattern of C/Si = 3.3:1 composite nanofiber.

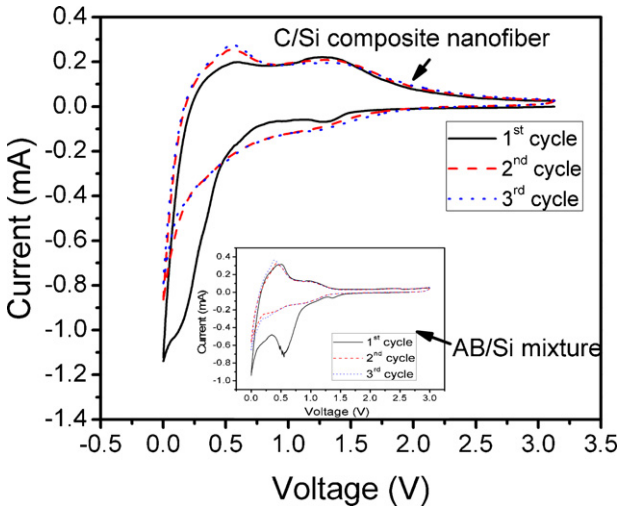

Fig. 4. Cyclic voltammogram of the first three cycles of C/Si = 3.3:1 composite nanofiber and the AB/Si = 3:1 mixture (inset picture). The scanning rate is 0.3 mV s^{-1} while in the electrochemical of 0–3.1 V.

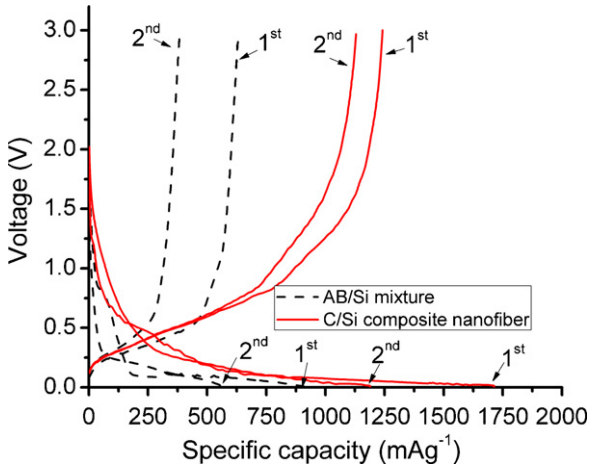

Fig. 5. Voltage profiles of the C/Si = 3.3:1 composite nanofiber and AB/Si = 3:1 mixture. The voltage cutoff is 0–3 V with current density of 0.1 C (1 C = 1500 mA g^{-1}).

fluctuation in capacity is observed in the first five cycles, and it should be related to the morphology change of the composite fiber, which will be discussed later. After five cycles, the fiber still has a high reversible capacity of more than 1150 mAh g^{-1}. As the current density is increased to 0.33 C, the capacity drops from 1150 to 870 mAh g^{-1} and then it is stabilized at around 750 mAh g^{-1}. During the subsequent cycles, the fiber exhibits good capacity retention with a slow fading. When the current density is decreased to 0.1 C again after 40 cycles, the capacity of the C/Si fiber also recovers to a high level up to 1100 mAh g^{-1}. It is also noticed that the columbic efficiency in 0.3 C is higher than that in 0.1 C. According to the results obtained from AgSn thin film electrode, the SEI may be damaged and then reformed during the charge/discharge process [21]. Therefore, the efficiency difference should be related to the different thickness and composition of SEI formed in different current densities. On the other hand, the electrode made of AB/Si mixture exhibits a very fast capacity fading and almost delivers no capacity after 10 cycles. This result is in agreement with Tarascon's early report [10]. Hence the electrochemical performance of the C/Si composite fibers benefits not only from the high content of carbon, but also from the well distribution of silicon particles and the fibrous morphology (Fig. 1b). There are a lot of spaces that can effectively buffer the strains resulting from the volume expansion/shrinkage during the lithium insertion/extraction. The adherence between the active materials (C/Si) and current collector becomes more stable compared with the electrode made of mechanically mixed silicon nanoparticles and carbon black, which results in better cycling performance.

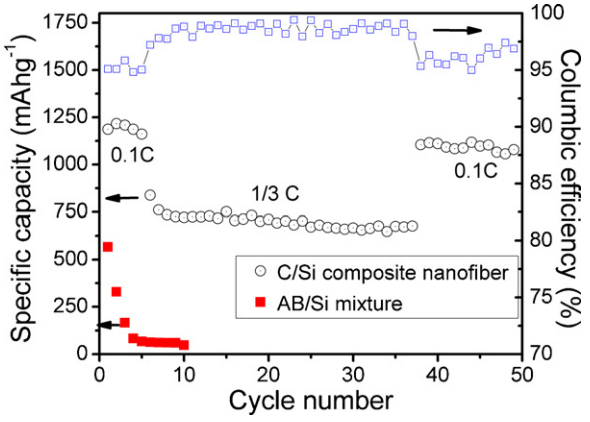

Fig. 6. Discharge capacity and columbic efficiency vs. cycle number of C/Si = 3.3:1 composite nanofiber and AB/Si = 3:1 mixture.

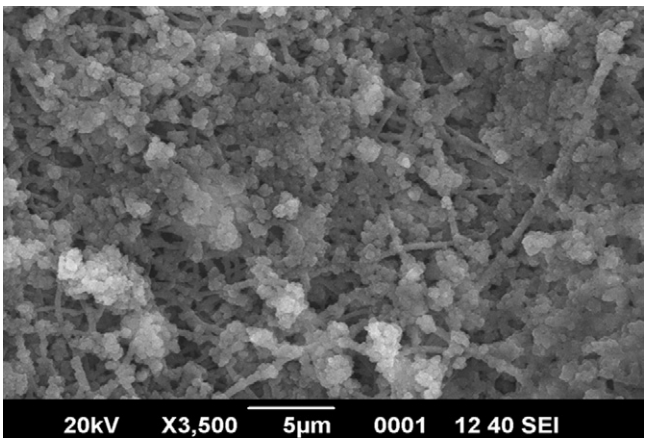

Fig. 7. Ex situ SEM picture of C/Si = 3.3:1 composite nanofiber cycled for 15 cycles at 0.1 C.

Though the cycling capability of the C/Si composite fiber is significantly enhanced compared with traditional carbon/silicon composite, there is still a capacity fade during the cycling, so it is necessary to examine the morphology change after several cycles. Also, the resistance change during lithium intercalation/deintercalation should be investigated to understand the large capacity drop when increasing the current density. Fig. 7 shows the ex situ SEM images of the C/Si composite fiber after 15 cycles. It can be clearly seen that the fibrous morphology changes significantly due to the volume expansion of silicon during lithium insertion. The surface of the electrode is composed of many small particles, below which there are still some nanofibers remaining. With such morphology, it is inevitable that partial active materials will fall off from the current collector, resulting in slow capacity fading during cycling. Nevertheless, there are still lots of macropores in the electrode which can buffer the strains generated in the discharge/charge process, and most of the active materials will not break off from the current collector. Therefore, the cycling capability is much better than that of a dense electrode. Unfortunately, there may be also some problem raised from this porous electrode structure. AC impedance spectra of carbon–silicon-composite nanofiber/Li half cell at states of full-charge and discharge are

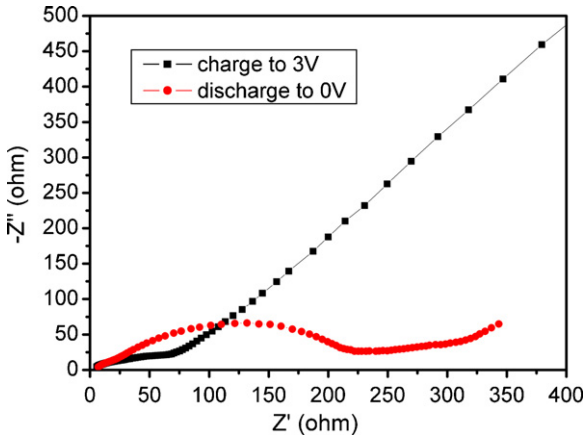

Fig. 8. AC impedance spectra of C/Si = 3.3:1 composite nanofiber. The measurement was conducted after three formation cycles.

shown in Fig. 8. It is noticed that when the cell is fully discharged to 0 V, the second semicircle of the spectra increases significantly (from less than 35 to 180 ohm). The resistance increase is likely related to the deposition of lithium on the surface of electrode [22]; the situation may be worse when we have a porous structured electrode. Though the limitation in rate capability of the C/Si nanofiber may become an obstacle for high power lithium-ion batteries, the high reversible capacity and stable capacity retention still have attractive potential applications in the high energy-density lithium-ion batteries.

4. Conclusions

A novel electrospun C/Si composite nanofiber with optimized silicon content is prepared and investigated as an anode material for lithium ion batteries. It is well demonstrated that the fibrous morphology and well distribution of silicon particles in carbon matrix can effectively enhance the electrochemical performance compared to mechanically mixed C/Si anode. The composite nanofiber exhibits large reversible capacity (1240 mAh g^{-1}) and stable capacity retention even in 40 cycles, which is very attractive for developing high energy-density lithium ion batteries. On the other hand, the limitations of the C/Si nanofiber are also discussed because its rate capability is not so satisfactory.

Acknowledgements

This study was supported by National Science Foundation of China (grant no. 20971117) and Education Department of Anhui Province (grant no. KJ2009A142). We are also grateful to the Solar Energy Operation Plan of Academia Sinica.

References

[1] W.J. Weydanz, M. Wohlfahrt-Mehrens, R.A. Huggins, J. Power Sources 81/82 (1999) 237.
[2] B.A. Boukamp, G.C. Lesh, R.A. Huggins, J. Elctrochem. Soc. 128 (1981) 725.
[3] J. Yang, M. Winter, J.O. Besenhard, Solid State Ionics 90 (1996) 281.
[4] M. Winter, J.O. Besenhard, M.E. Spahr, P. Novak, Adv. Mater. 10 (1998) 725.
[5] C.K. Chan, H.L. Peng, G. Liu, K. Mcilwrath, X.F. Zhang, R.A. Huggins, Y. Cui, Nat. Nanotechnol. 3 (2008) 31.
[6] L.F. Cui, R. Ruffo, C.K. Chan, H.L. Peng, Y. Cui, Nano Lett. 9 (2009) 491.
[7] N. Dimov, S. Kugino, M. Yoshio, Electrochim. Acta 48 (2003) 1579.
[8] Z.S. Wen, J. Yang, B.F. Wang, K. Wang, Electrochem. Commun. 5 (2003) 165.
[9] T. Hasegawa, S.R. Mukai, Y. Shirato, H. Tamon, Carbon 42 (2004) 2573.
[10] J. Saint, M. Morcrette, D. Larcher, L. Laffont, S. Beattie, J.P. Peres, D. Talaga, M. Couzi, J.M. Tarascon, Adv. Funct. Mater. 17 (2007) 1765.
[11] S.H. Ng, J.Z. Wang, D. Wexler, K. Konstantinov, Z.P. Guo, H.K. Liu, Angew. Chem. Int. Ed. 45 (2006) 6869.
[12] Z.J. Luo, D.D. Fan, X.L. Liu, H.Y. Mao, C.F. Yao, Z.Y. Deng, J. Power Sources 189 (2009) 16.
[13] H. Wolf, Z. Pajkic, T. Gerdes, M. Willert-Porada, J. Power Sources 190 (2009) 157.
[14] L. Wang, Y. Yu, P.C. Chen, D.W. Zhang, C.H. Chen, J. Power Sources 183 (2008) 717.
[15] L. Wang, Y. Yu, P.C. Chen, C.H. Chen, Scr. Mater. 58 (2008) 405.
[16] C. Kim, K.S. Yang, M. Kojiama, K. Yoshida, Y.J. Kim, Y.A. Kim, M. Endo, Adv. Funct. Mater. 16 (2006) 2393.
[17] A.T. Serkov, Fibre Chem. 39 (2007) 60.
[18] H. Li, X.J. Huang, L.Q. Chen, Z.G. Wu, Y. Liang, Electrochem. Solid-State Lett. 2 (1999) 547.
[19] S. Kim, P.N. Kumata, J. Power Sources 136 (2004) 145.
[20] Y.P. Wu, C.R. Wan, C.Y. Jiang, S.B. Fang, Y.Y. Jiang, Carbon 37 (1999) 1901.
[21] D.T. Shieh, J.T. Yin, K. Yamamoto, M. Wada, S. Tanase, T. Sakai, J. Electrochem. Soc. 153 (2006) A106.
[22] N. Ding, J. Xu, Y.X. Yao, G. Wegner, X. Fang, C.H. Chen, I. Lieberwirth, Solid State Ionics 180 (2009) 222.